Int J Cardiovasc Imaging (2012) 28:7–13
DOI 10.1007/s10554-012-0072-y

ORIGINAL PAPER

Triple rule-out acute chest pain evaluation using a 320-row-detector volume CT: a comparison of the wide-volume and helical modes

Eun-Ju Kang · Ki-Nam Lee · Dong Won Kim · Bo Sung Kim · Sunseob Choi · Byeong-Ho Park · Jong Young Oh

Received: 29 April 2012 / Accepted: 10 May 2012 / Published online: 23 May 2012

Abstract The purpose of this study was to investigate the image quality and radiation dose of triple rule-out computed tomography (TROCT) using a 320-row-detector volume CT system to compare the wide-volume and helical modes of this CT system. Sixty-four patients with non-critical chest pain were allocated to one of 2 groups according to the type of CT examination mode used. Group 1 patients were examined using the wide-volume (non-spiral) mode and group 2 patients were examined using the 160-detector row helical mode, with the same contrast injection protocol in both methods [biphasic injection protocol; injection rate of 4 ml/s, median volume, 70 ml (range 65–100 ml)]. Attenuations of the pulmonary trunk, ascending aorta, and coronary arteries were measured in Hounsfield units; a subjective overall patient-based image quality score of 1–3 was awarded to each study. Effective doses, signal-to-noise ratio (SNR) and contrast-to-noise ratio (CNR) were calculated. Average effective dose was significantly lower in group 1 than group 2 (9.7 ± 5.1 vs. 16 ± 5.9 mSv, $P < 0.001$). The mean attenuation of the main pulmonary trunk was significantly higher in group 1 than group 2 ($P = 0.04$) and mean attenuations in other vessels were not significant different. SNR and CNR were not significantly different between the groups. The proportion of diagnostic image qualities for chest CT angiography (CTA) was similar between the groups (93.5 vs. 93.9 %). In coronary CTA, group 1 showed a higher proportion of diagnostic image qualities than group 2 (100 vs. 87.9 %). The use of wide-volume mode of 320-detector CT reduces the overall effective radiation dose and results in similar attenuation and image quality for TROCT as compared with the helical mode.

Keywords Computed tomography · Chest pain · Radiation exposure · Thorax

E.-J. Kang · K.-N. Lee (✉) · D. W. Kim · B. S. Kim · S. Choi · B.-H. Park · J. Y. Oh
Department of Radiology, Dong-A University College of Medicine, 1, 3-ga Dongdaesin-dong, Seo-gu, Busan 602-715, Republic of Korea
e-mail: gnlee@dau.ac.kr

Introduction

Acute-onset chest pain is one of the most frequent symptoms encountered in the emergency department (ED), and accounts for 5–20 % of visits to ED [1]. However, evaluating the causes of chest pain in ED is one of the most difficult challenges for physicians, because many diseases can cause chest pain. Triple rule-out computed tomography (TROCT) can provide a cost-effective means of evaluating coronary arteries, the aorta, and pulmonary arteries in patients with acute chest pain [2, 3]. However, the longer anatomical coverage is required than coronary CT angiography (CTA). All TRO protocols require sufficient and simultaneous opacification of pulmonary arteries, coronary arteries, and aorta, which results in larger radiation exposures and large doses of contrast medium [2–4]. Several strategies such as a low kVp protocol or high-pitch spiral dual-source CT technique have been used to minimize radiation dose for TROCT protocols [5, 6]. A 320-detector-row CT provides the largest z-axis coverage of 16 cm, and thus, allows 3-dimensional volumetric, whole heart image capture during one RR interval of a cardiac cycle. By using this scanner, the whole chest CTA scan can be achieved with 2 axial volume scan acquisitions ("wide-volume scan"), which reduces the duration of CT acquisition and radiation exposure [7]. Therefore, we undertook this study

to investigate the image quality and radiation dose required TROCT using a wide-volume scan mode and to compare this with a helical mode on the same CT system.

Materials and methods

Patients

In this prospective study conducted at a single center, 64 patients (47 males and 17 females; age range, 19–85 years; mean age, 60.1 ± 15.1 years) were consecutively enrolled. Inclusion criteria were; the presence of an acute (but noncritical) pain, clinical suspicion of pulmonary embolism, aortic dissection, or low-to-intermediate risk of coronary artery disease (CAD). The exclusion criteria applied were a high risk for CAD, a history of allergic reaction to contrast material, and renal insufficiency. In all patients, a nitroglycerin spray (2 puffs) was administered sublingually, and when the heart rate was >65 beats per minute (bpm) beta-blocking agents were administered if not contraindicated. The patients were randomly allocated to 2 different TRO protocols: 31 to wide-volume scan (non-spiral) mode (group 1), and 33–160-detector row helical mode (group 2; the control group).

Image acquisition and post-processing

All 64 patients underwent TROCT on a 320-detector-row scanner (Aquilion ONE, Toshiba Medical Systems, Otawara, Japan) with 320 × 0.5 mm collimation; 350-ms gantry rotation time; 175-ms temporal resolution. Tube voltage and current were modulated by body mass index (BMI); tube voltages were set to either 100 or 120 kVp and tube current ranged 400–550 mA (Table 1).

Nonionic contrast material (iobitridol, Xenetix® 350 mgI/ml; Guerbet, France) was administrated intravenously at 4 ml/s (median amount, 70 ml; range 65–100 ml) followed by 30 ml of a contrast–saline mixture (2:8 dilution) at 4 ml/s, which was the same as the routine coronary CTA protocol used at our institution. CT scans covered the entire thoracic aorta from the clavicle to the base of the heart.

All TROCT scans were started using automatic bolus triggering at 1 s intervals in the ascending aorta [the triggering level was 90 HU (Hounsfield units)] with a delay of 5 s, by craniocaudal direction. Wide-volume (non-spiral) mode chest CTA in group 1 patients consisted of acquiring 2 data points with a 4–5 s interval between acquisitions due to a mechanical limitation. The detector width was set at 14–16 cm to cover half of the entire thorax. The resulting thin-slice partial volume data sets were automatically stitched immediately after reconstruction for a chest examination. A second dataset (lower part of chest) was separately reconstructed for coronary CTA (Fig. 1). Group 2 patients were imaged in a 160-detector row helical mode at a detector width of 8 cm and 0.17–0.25 pitch. The resulting datasets were reconstructed for chest CTA and coronary CTA, respectively.

When the heart rate was sufficiently slow (≤65 bpm), CT scans were obtained by prospectively triggered 70–80 % data acquisition of the RR interval (groups 1A and 2A). The examinations of other patients (group 1B and 2B) were performed by retrospective data acquisition with ECG-based tube current modulation, because the heart rates of these patients were >65 bpm despite beta-blocker administration. In some patients in group 1B with rapid, irregular heartbeats, the images were produced using multisegment reconstruction of 2 heartbeats.

Axial images of the whole thorax scan range were reconstructed from 75 % of RR interval at a slice thickness of 3 mm. In addition, heart regions were reconstructed in a field of view adapted to heart size at a slice thickness of 0.5 mm, and an initial interpretation was performed using reconstructed images from the 75 % of RR interval or the automatically suggested 'best phase (ms)'. Additional systolic or diastolic phase images were reconstructed in patients with rapid heartbeats, as needed. All data sets were transferred to a Vitrea Workstation (Vital images, MN, USA) for image analysis.

Analysis of image noise and quality

The attenuations (HU) of the main pulmonary artery, ascending aorta, and coronary arteries (proximal left anterior descending artery, proximal left circumflex artery and proximal right coronary artery) on each axial image were measured. Regions of interest (ROI) used for these measurements were chosen to be as large as possible, and calcifications and plaques were carefully avoided. Signal-to-noise ratio (SNR) and contrast-to-noise ratio (CNR) in

Table 1 Reference tube potential and tube current according to body mass index

BMI	≤17	18–19	20–21	22–23	24–25	26–30	31–35	36–40	>40
kV	100	100	100	100	120	120	120	120	135
mA	450	500	520	550	400	450	500	580	510

kV tube potential, *mA* tube current, *BMI* body mass index

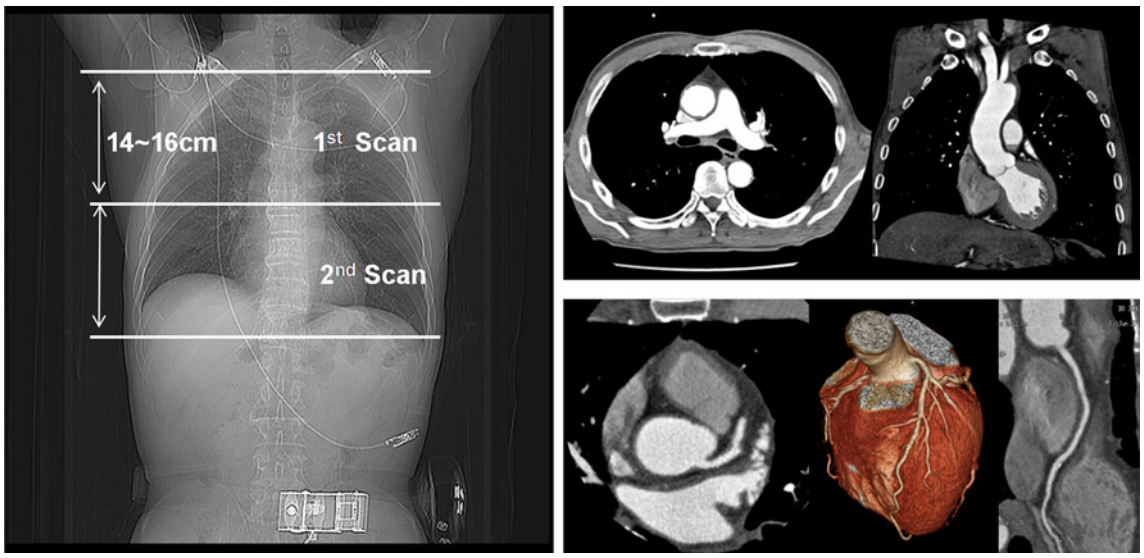

Fig. 1 A schematic showing the wide-volume scan method. Whole chest CT scan archived with 2 acquisitions of axial volume scan that were automatically stitched immediately after reconstruction (*right upper*) than the second data (*lower portion* of chest) were separately reconstructed for coronary angiography (*right lower*)

the proximal right coronary artery (RCA) were calculated as previously published [8, 9]. Vessel contrast was calculated as the difference between the mean attenuation of contrast medium in a contrast-enhanced vessel lumen and the mean attenuation in an adjacent perivascular tissue. Image noise was defined as the standard deviation (SD) of the attenuation value of the ROI placed in the aortic root. Based on these measurements, SNR and CNR were calculated using the following equations:

$$\mathrm{SNR} = \mathrm{Vessel\ density}\left(\mathrm{HU}^{\mathrm{ascending\ aorta}}\right)/ \mathrm{Image\ noise}\left(\mathrm{SD}^{\mathrm{ascending\ aorta}}\right),$$

$$\mathrm{CNR} = \mathrm{Vessel\ contrast}\left(\mathrm{HU}^{\mathrm{RCA}} - \mathrm{HU}^{\mathrm{perivascular\ tissue}}\right)/ \mathrm{Image\ noise}\left(\mathrm{SD}^{\mathrm{ascending\ aorta}}\right).$$

To determination image qualities, a subjective overall patient-based image quality score of 1–3 was assigned to the coronary CTA and chest CTA in each study. Quality scores were defined as follows: 1 = excellent, no motion artifact and excellent visualization of vessel lumen; 2 = good, some artifact, but still sufficient for diagnosis; and 3 = poor; massive motion artifacts, inadequate for diagnosis.

Estimation of radiation dose

The products of CT dose index (CTDIvol) and scan lengths were calculated, and effective doses (mSv) were calculated as described by the European Working Group guidelines regarding Quality Criteria for CT using the dose–length product and a conversion coefficient (k = 0.017 mSv/[mGy cm]) [10].

Statistics

TROCT in 160-detector row helical mode was defined as the standard protocol. All estimated data (radiation dose used during each examination, HU, SNR and CNR) were expressed as mean ± SD. PASW® Statistics 18 (SPSS Inc., Chicago, IL, USA) was used for the statistical analysis. Differences between groups were examined using independent *t* tests for continuous variables and the χ^2 test for categorical variables, and *P* values of less than 0.05 were considered statistically significant.

Results

No significant difference in age, gender distribution, body-mass index (BMI), or heart rate was evident between groups 1 and 2 (Table 2). A total of 26 patients (12 patients in group 1 and 14 patients in group 2) underwent TROCT at 100 kVp. Two patients in each group experienced arrhythmia; images of these patients were produced with retrospective mode of each protocol.

The vessel density of the pulmonary artery, ascending aorta and coronary arteries were excellent and sufficient for diagnosis in all 64 examinations. The mean attenuation of the main pulmonary trunk was higher in group 1 than in group 2 (379.2 ± 142.1 HU vs. 312.6 ± 104.6 HU; $P = 0.04$) and that of other vessels (ascending aorta and coronary arteries) were not significantly different in the 2 groups (Table 3). Image noise (SD of the ascending aorta) was not significantly different between the 2 groups (32.8 ± 7.9 vs. 33.5 ± 8.7; $P = 0.74$). There were no

Table 2 General characteristics of patients

Groups	Wide-volume mode (group 1)			Helical mode (group 2)			Total (*P* value)
	1A	1B	Total group 1	2A	2B	Total group 2	
Number of patients	19	12	31	21	12	33	64
100 kV	6	6	12	8	6	14	26
120 kV	13	6	19	13	6	19	38
Sex (male/female)	14/5	8/4	22/9	19/2	6/6	25/8	47/17
Age (years)	60 ± 12.3	60 ± 18.9	60 ± 14.9	56 ± 15.7	66 ± 13.8	60 ± 15.6	60.1 ± 15.1 (0.93)
BMI (kg/m^2)	22.9 ± 2.1	22.4 ± 2.0	22.7 ± 2.0	23.0 ± 2.5	23.1 ± 2.6	23.5 ± 3.0	23.1 ± 2.6 (0.20)
Heart rate (bpm)	59 ± 10.6	68 ± 12	62 ± 12.1	57 ± 4.9	65 ± 10.6	60 ± 8.4	61.0 ± 10.3 (0.33)

Values are presented as mean ± SD

BMI body mass index, *1A* prospective wide volume mode, *1B* retrospective wide volume mode, *2A* prospective helical mode, *2B* retrospective helical mode

Table 3 Comparison of two acquisition modes for mean attenuation of each vessel, background noise, signal-to-noise ratio, and contrast-to-noise ratio

	Wide-volume mode (group 1, $n = 31$)	Helical mode (group 2, $n = 33$)	Total ($n = 64$)	*P*
Density of vessels (HU)				
Pulmonary trunk	379.2 ± 142.1	312.6 ± 104.6	344.3 ± 127.3	0.04
Ascending aorta	451.8 ± 95.3	453.9 ± 94.4	452.9 ± 94.0	0.93
LAD	435.2 ± 104.7	410.8 ± 78.1	423.0 ± 92.3	0.35
RCA	444.8 ± 121.0	446.8 ± 57.6	445.8 ± 92.6	0.93
LCX	439.5 ± 113.8	422.6 ± 99.8	431.2 ± 106.5	0.58
Background noise (HU)	32.8 ± 7.9	33.5 ± 8.7	33.2 ± 8.2	0.74
SNR	13.6 ± 4.4	14.1 ± 4.9	13.9 ± 4.7	0.70
CNR	16.8 ± 4.5	16.5 ± 4.6	16.7 ± 4.5	0.80

Values are presented as mean ± SD

HU Hounsfield unit, *LAD* left anterior descending artery, *RCA* right coronary artery, *LCX* left circumflex artery, Background noise means SD of aortic root, *SNR* signal-to-noise ratio, *CNR* contrast-to-noise ratio

significant differences between groups 1 and 2, respectively for SNR (13.6 ± 4.4 vs. 14.1 ± 4.9; $P = 0.70$) and CNR (16.8 ± 4.5 vs. 16.5 ± 4.6; $P = 0.80$) (Table 3).

Assessment of subjective image quality on axial images for chest CTA and multiplanar reconstruction images for coronary CTA revealed an overall diagnostic image quality (score 1 and 2) of 93.7 % for both chest CTA and coronary CTA (Table 4). On chest CTA, the group 2 showed a larger image number with excellent quality (score 1; 67.7 vs. 87.9 %, respectively, $P = 0.09$), but no significant difference regarding the range of diagnostic image quality (score 1 and 2; 93.5 vs. 93.9 %, respectively) and the number of patients with poor image quality (score 3; 6.5 vs. 6.1 %, respectively) as compared with group 1. In coronary CTA, there were no significant differences in the number of patients with excellent quality (score 1; 77.4 vs. 75.8 %, respectively) between the 2 groups, but poor image quality (score 3) were observed only in group 2 (4 of 33 images, 12.1 %, $P = 0.09$) (Table 4). Two patients in each group showed poor quality (score 3) of chest CTA, due to breathing artifacts. The chest CTA of 2 patients in group 1B showed stair-step artifacts occurring between the 2 axial volume scans, but the coronary CTA was still of diagnostic quality (Fig. 2a). The chest CTA in 2 patients of group 2B showed multiple stair-step artifacts, and in these patients, coronary CTA image quality was also non-diagnostic (Fig. 2b).

The wide-volume scan mode TROCT protocol required a lower radiation dose than the 160-raw standard helical protocol (Table 5). Mean scan length was greater in group 1 than in group 2 (26.3 ± 20.5 vs. 23.8 ± 3.3 cm, respectively; $P = 0.0005$), but the average effective dose was significantly lower in group 1 than in group 2 (9.7 ± 5.1 vs. 16.1 ± 6.0 mSv, respectively; $P < 0.0001$).

Table 4 Qualitative assessment of image quality for chest CTA and coronary CTA in each group

	Wide-volume mode (group 1, $n = 31$)	Helical mode (group 2, $n = 33$)	Total ($n = 64$)
Chest CTA			
Excellent (1)	21/31 (67.7 %)	29/33 (87.9 %)	50/64 (78.1 %)
Diagnostic (1 + 2)	29/31 (93.5 %)	31/33 (93.9 %)	60/64 (93.7 %)
Poor (3)	2/31 (6.5 %)	2/33 (6.1 %)	4/64 (6.3 %)
Coronary CTA			
Excellent (1)	24/31 (77.4 %)	25/33 (75.8 %)	49/64 (76.6 %)
Diagnostic (1 + 2)	31/31 (100 %)	29/33 (87.9 %)	60/64 (93.7 %)
Poor (3)	0/31 (0 %)	4/33 (12.1 %)	4/64 (6.3 %)

Values are presented as number of cases (%)

CTA CT angiography, images score; 1 = excellent, no motion artifact, 2 = good, some artifact, but still sufficient for diagnosis, 3 = poor, inadequate for diagnosis

Fig. 2 Two cases of patients who showed poor image quality of chest CTA, due to breathing artifacts. **a** A 40-year-old man (in group 1B) underwent the wide-volume method TROCT. The chest CTA showed stair-step artifact (*arrow* in **a**) between the 2 volume scans, but the image quality of coronary CTA was diagnostic. **b** A 35-year-old man (in group 2B) underwent retrospective helical method TROCT. The chest CTA showed multiple stair-step artifacts (*arrows* in b) at whole chest and coronary CTA was also non-diagnostic

Two patients of group 1B (wide-volume retrospective mode) showed rapid, irregular heartbeats despite beta blocker administration (86–92 and 75–86 bpm, respectively), and thus, images were obtained with a multisegment reconstruction method using 2 heartbeats (Fig. 3). In these patients, images were diagnostic, but a large effective dose was produced (23.2 and 25.1 mSv, respectively).

Discussion

The comprehensive evaluation of the coronary arteries, aorta, and the pulmonary vasculature, is critically important in patients with acute chest pain. However, the visualization of different vascular territories in the entire chest, during a single examination, is a major challenge. Probably

Table 5 Comparison of radiation doses between two groups

Groups	Wide-volume mode (group 1, $n = 31$)			Helical mode (group 2, $n = 33$)			Total (P value)
	1A	1B	Total group 1	2A	2B	Total group 2	
Exposure time (s)	0.76 ± 0.2	3.14 ± 0.9	1.68 ± 1.3	3.39 ± 1.1	8.05 ± 1.8	5.08 ± 2.6	3.44 ± 2.7 (<0.0001)
CTDIvol (mGy)	18.0 ± 4.0	38.9 ± 15.0	26.1 ± 14.1	28.9 ± 5.0	57.9 ± 9.6	39.5 ± 15.7	33.0 ± 16.3 (0.0007)
Scan length (cm)	26.4 ± 2.0	26.3 ± 2.1	26.3 ± 20.5	24.6 ± 2.7	22.4 ± 3.7	23.8 ± 3.3	25.1 ± 2.9 (0.0005)
Effective dose (mSv)	6.8 ± 1.7	14.4 ± 5.2	9.7 ± 5.1	12.3 ± 2.4	22.8 ± 3.4	16.1 ± 6.0	13.0 ± 6.4 (<0.0001)
100 kV	5.7 ± 2.4	11.6 ± 3.3	8.7 ± 4.1	12.7 ± 2.7	20.8 ± 3.1	16.2 ± 5.0	
120 kV	7.3 ± 1.0	17.3 ± 5.4	10.4 ± 5.6	12.0 ± 2.4	24.8 ± 3.6	16.0 ± 6.6	

Values are presented as mean ± SD

CTDIvol CT dose index, *1A* prospective wide volume mode, *1B* retrospective wide volume mode, *2A* prospective helical mode, *2B* retrospective helical mode

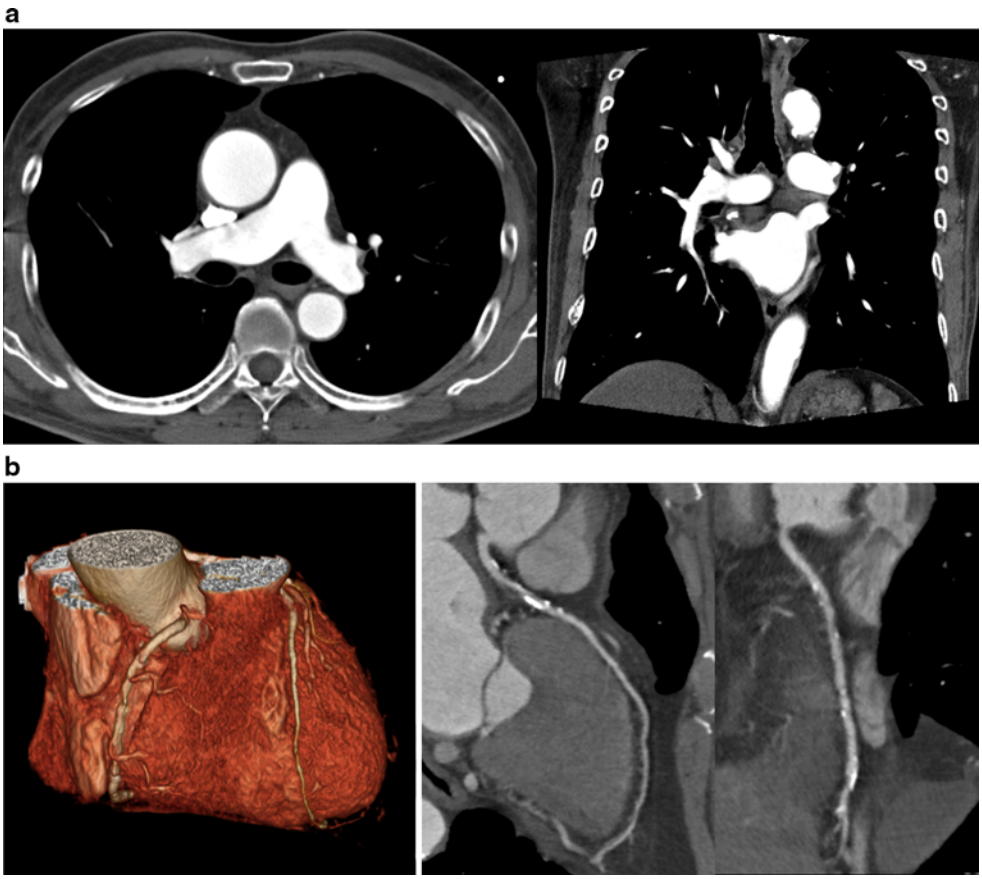

Fig. 3 A case of group 1B underwent TROCT with multisegment reconstruction method. The patient was an 88-year-old man with rapid and irregular heartbeats (86–92 bpm). Both chest CTA (**a**) and coronary CTA (**b**) images were diagnostic in quality (exposure time, 4.3 s; CTDIvol, 62.2 mGy; scan length, 26.4 cm; effective doses, 23.2 mSv)

the most critical issues regarding the TROCT protocol are adequacy of contrast enhancement in the thoracic vessels and radiation dose. Various CT techniques have been proposed to reduce radiation dose and contrast amounts for TROCT, to dates. Krissak et al. [5] reported that the use of a low kVp protocol in non-obese (BMI $\leq$ 25 kg/m^2) patients produced diagnostic imaging quality with significantly reduced radiation dose, as has been reported by several authors for coronary CTA studies [11, 12]. However, in patients with a higher BMI, a lower kVp protocol leads to higher image noise and in the worst case scenarios it may produce non-diagnostic images [13]. Sommer et al. [6] described a dose-saving TROCT method based on the use of a prospective ECG-gating high-pitch dual spiral technique for patients with heart rates below 65 bpm. However, this method is not suitable in patients with rapid

(>65 bpm) or variable heartbeats, especially in an emergency situation. Durmus et al. [7] recently published an article on a low-dose TRO protocol using a 320-row-detector CT, which resulted in excellent opacification of vessels and image quality with reduction of contrast medium. However, this study only included patients with a body weight below 90 kg; a BMI below 30; and a heart rate below 65 bpm. In the present study, we used a 320-detector CT for TROCT in all included patients without any exclusion for heartbeat rates or BMI. Furthermore, we compared wide-volume scan method with a 160-raw helical method for image quality and radiation dose. To the best of our knowledge, no other similar study has been published in the English literature.

In our study, mean scan length was longer for wide-volume than helical mode scans. This might happen, because, in wide-volume mode, the detector width could be changed only in increments of 2 cm (12, 14 or 16 cm), but in helical mode, the detector width could be altered more minutely. However, the mean effective radiation dose was significantly lower for wide-volume scan mode than standard helical mode. The mean exposure time of wide-volume scans was less than a third of that of helical scans. Therefore, by using wide-volume scans, we were able to reduce radiation doses, and achieve greater opacification of pulmonary arteries using the same amount of contrast media.

The wide-volume method showed less proportion of excellent quality score of chest CTA than that of helical method, because of the relatively long time intervals (4–5 s) between 2 volume scans that produced stair-step artifacts or a difference in vessel densities. However, most of wide-volume chest CTA images were acceptable for diagnosis without significant data loss, and all coronary CTA had a diagnostic quality score. Thus, we propose wide-volume TROCT in the patient with symptoms that are more suspicious for coronary origin chest pain than for aortic or pulmonary artery disease.

The usefulness of the multisegment reconstruction method has been well studied by many authors [14, 15]. In the present study, this method allowed us to obtain diagnostic images in patients with rapid or irregular heartbeats, although radiation doses in these patients were significantly higher than those in other patients.

Some limitations of this study deserve consideration. First, the number of patients included was relatively small. Second, the study was performed on one CT scanner and results obtained using CT scanners of other manufacturers are likely to differ. Third, we could not assess the diagnostic accuracies of our protocols, because only a small number of patients underwent conventional angiography.

In conclusion, the use of wide-volume mode reduces overall effective radiation doses by around 60 % and results in similar opacification of thoracic arteries and image quality for triple rule-out CT, as compared with the helical mode. Even for patients with rapid and irregular heartbeats, wide-volume scans mode may produce coronary CTA of diagnostic quality.

Acknowledgments This study was supported by research funds from Dong-A University.

Conflict of interest None.

References

1. Karlson BW, Herlitz J, Pettersson P et al (1991) Patients admitted to the emergency room with symptoms indicative of acute myocardial infarction. J Intern Med 230(3):251–258
2. Ladapo JA, Hoffmann U, Bamberg F et al (2008) Cost-effectiveness of coronary MDCT in the triage of patients with acute chest pain. AJR Am J Roentgenol 191(2):455–463
3. Frauenfelder T, Appenzeller P, Karlo C et al (2009) Triple rule-out CT in the emergency department: protocols and spectrum of imaging findings. Eur Radiol 19(4):789–799
4. Schertler T, Frauenfelder T, Stolzmann P et al (2009) Triple rule-out CT in patients with suspicion of acute pulmonary embolism: findings and accuracy. Acad Radiol 16(6):708–717
5. Krissak R, Henzler T, Prechel A et al. (2010) Triple-rule-out dual-source CT angiography of patients with acute chest pain: dose reduction potential of 100 kV scanning. Eur J Radiol. doi: 10.1016/j.ejrad.2010.11.021
6. Sommer WH, Schenzle JC, Becker CR et al (2010) Saving dose in triple-rule-out computed tomography examination using a high-pitch dual spiral technique. Invest Radiol 45(2):64–71
7. Durmus T, Rogalla P, Lembcke A et al (2011) Low-dose triple-rule-out using 320-row-detector volume MDCT—less contrast medium and lower radiation exposure. Eur Radiol 21(7):1416–1423
8. Husmann L, Alkadhi H, Boehm T et al (2006) Influence of cardiac hemodynamic parameters on coronary artery opacification with 64-slice computed tomography. Eur Radiol 16(5):1111–1116
9. Lembcke A, Wiese TH, Schnorr J et al (2004) Image quality of noninvasive coronary angiography using multislice spiral computed tomography and electron-beam computed tomography: intraindividual comparison in an animal model. Invest Radiol 39(6):357–364
10. European Commission (2000) European guidelines on quality criteria for computed tomography, EUR 16262 EN. Office for Official Publications of the European Communities, Luxembourg
11. Feuchtner GM, Jodocy D, Klauser A et al (2010) Radiation dose reduction by using 100-kV tube voltage in cardiac 64-slice computed tomography: a comparative study. Eur J Radiol 75(1):e51–e56
12. Pflederer T, Rudofsky L, Ropers D et al (2009) Image quality in a low radiation exposure protocol for retrospectively ECG-gated coronary CT angiography. AJR Am J Roentgenol 192(4):1045–1050
13. Huda W, Scalzetti EM, Levin G (2000) Technique factors and image quality as functions of patient weight at abdominal CT. Radiology 217(2):430–435
14. Dewey M, Teige F, Laule M et al (2007) Influence of heart rate on diagnostic accuracy and image quality of 16-slice CT coronary angiography: comparison of multisegment and halfscan reconstruction approaches. Eur Radiol 17(11):2829–2837
15. Schnapauff D, Teige F, Hamm B et al (2009) Comparison between the image quality of multisegment and halfscan reconstructions of non-invasive CT coronary angiography. Br J Radiol 82(984):969–975